

FIBRE OPTICS

PACS numbers: 42.55.Wd; 42.81.Dp
DOI: 10.1070/QE2004v034n09ABEH002688

Lasing parameters of ytterbium-doped fibres doped with P_2O_5 and Al_2O_3

M.A. Melkumov, I.A. Bufetov, K.S. Kravtsov, A.V. Shubin, E.M. Dianov

***Abstract*. Absorption and emission cross sections are measured for the $^2F_{5/2} \rightarrow {}^2F_{7/2}$ transition in Yb^{3+} ions in silica fibres doped with Al_2O_3 and P_2O_5. The measurements were performed by methods based on spectroscopic data and by more direct methods based on laser-transition saturation. Possible lasing ranges of ytterbium-doped double-clad fibre lasers are calculated from the measured spectral dependences of stimulated transition cross sections.**

Keywords: *stimulated transmission cross section, fibre laser, double-clad fibre*.

1. Introduction

Silica optical fibres are perfect media for doping with Yb^{3+} ions for fabrication of fibre lasers and amplifiers. At present efficient ytterbium-doped fibre amplifiers and lasers with output powers from a few watts to a few kilowatts have been developed (see, for example, [1 – 5] and references therein). The development of such devices involves preliminary numerical simulation and optimisation of their parameters. However, information on laser transition cross sections for ytterbium ions in silica glasses used for fabrication of optical fibres available in the literature is scarce so far. Thus, the spectral dependences of the absorption and stimulated emission cross sections for ytterbium ions in a germanosilicate glass were presented only in papers [1, 2] (however, the glass composition was not indicated). The composition of Yb^{3+}-doped glasses studied in [6 – 8] differs strongly from that of the core of fibres studied in this paper. Since it has been shown in all studies that transition cross sections strongly depend on the glass composition, the data reported in the literature cannot be used in most cases to simulate fibre lasers. In addition, a comparison of results obtained for bulk samples and fibres suggests that the measurements of stimulated emission cross sections measured for ytterbium ions in bulk samples may be incorrect because of radiation reabsorption.

At present two types of ytterbium fibres are mainly used in fibre lasers: silica fibres with the core doped with P_2O_5 [phosphosilicate (PS) fibres] or doped with Al_2O_3 and a small amount of GeO_2 [alumosilicate (AS) fibres]. The dopants P_2O_5, Al_2O_3, and GeO_2 are required to form an appropriate profile of the refractive index of the fibre, to provide homogeneous doping of the glass matrix with Yb, to eliminate clustering, and to reduce optical losses in the fibre.

In this paper, we studied a number of PS fibres with mass content of phosphorus and ytterbium in the fibre core in the range 4 % – 10 % and 1 % – 8 %, respectively. The mass content of aluminium and ytterbium was 1 % – 2 % and 1 % – 3 %, respectively. The fibre preforms were fabricated by the MCVD method. Ytterbium and aluminium were doped into AS fibres and ytterbium was doped into PS fibres using the solution technology (for some samples) or from a gas phase (for other samples). Our measurements did not reveal noticeable differences between transition cross sections for fibres of each type (PS or AS), irrespective of the concentration of dopants in the regions indicated above and of the method of doping (from solution or gas phase). However, PS and AS fibres had substantially different characteristics. Therefore, below we will indicate only the fibre type, omitting its parameters.

We measured the spectral dependences of absorption and emission cross sections for the $^2F_{5/2} - {}^2F_{7/2}$ transition of Yb^{3+} ions doped to the core of PS and AS fibres. The system of levels of ytterbium ions in glass can be treated as a quasi-two-level one (despite the fact that each of the levels is split into sublevels in a crystal field) if the thermodynamically equilibrium distribution of populations over the sublevels is established in each multiplet. However, due to the description of this system as a two-level one, the absorption cross section σ_a and the stimulated emission cross section σ_e prove to be substantially different functions of the wavelength [9], which in turn depend on the form of the thermodynamic distribution of ions over sublevels, i.e., on temperature. In this paper, we consider in most cases the functions $\sigma_a(\lambda)$ and $\sigma_e(\lambda)$ at room temperature ($T \approx 293$ K), if temperature is not indicated.

Based on the data obtained, we calculated spectral ranges where lasing can be obtained in ytterbium-doped double-clad AS and PS fibres using Bragg gratings of the refractive index as mirrors.

M.A. Melkumov, I.A. Bufetov, K.S. Kravtsov, A.V. Shubin, E.M. Dianov Fiber Optics Research Center, A.M. Prokhorov General Physics Institute, Russian Academy of Sciences, ul. Vavilova 38, 119991 Moscow, Russia; Tel.: (095) 132 82 56; Fax: (095) 135 81 39; e-mail: iabuf@fo.gpi.ru

Received 9 April 2004; revision received 2 June 2004
Kvantovaya Elektronika **34** (9) 843 – 848 (2004)
Translated by M.N. Sapozhnikov

2. Measurement of stimulated transition cross sections

Laser transition cross sections for rare-earth ions in glasses and optical fibres can be measured by a variety of methods (see, for example, [10]). Methods used for measuring cross sections for rare-earth ions of a certain type (for example, Er^{3+}) are often applicable for measuring cross sections for other rare-earth ions. Compared to bulk samples, an important factor in the measurements of cross sections in fibres is the field inhomogeneity in the fibre core and, as a rule, the inhomogeneous distribution of active ions over the fibre radius. This circumstance complicates the measurements of transition cross sections in fibres.

We measured stimulated transition cross sections in ytterbium-doped single-mode AS and PS fibres with the core diameter of $6-8$ μm and the second-mode cutoff wavelength of ~ 1 μm. The cross sections were measured by several independent methods to improve the reliability of the results. We measured the spectral dependences of the absorption $\sigma_a(\lambda)$ and stimulated emission $\sigma_e(\lambda)$ cross sections in the wavelength range from 850 to 1200 nm and compared the spectral dependence of the $\sigma_e(\lambda)/\sigma_a(\lambda)$ ratio with the theoretical dependence obtained by McCumber [9]. The methods of cross-section measurement are described in detail in [11].

Absorption cross sections in fibres were measured by the methods described, for example, in [10] and [12], which are based on: (i) the small-signal absorption measuring in the fibre (small-signal absorption method), which gives the spectral dependence of the absorption cross section $\sigma_a(\lambda)$, and (ii) observation of luminescence saturation with increasing pump power (luminescence saturation method). The second method allows one to measure the value of $\sigma_a(\lambda)$ at a certain pump wavelength. The calibration of the absorption spectrum relative to the value of $\sigma_a(\lambda)$ at a given point gives the spectral dependence of the absorption cross section.

Different methods impose different requirements on the type of needed measurements. Thus, the small-signal absorption method requires the knowledge of the absolute values of the distribution of concentration of Yb^{3+} ions over the fibre core radius and the profile of the radiation intensity distribution over the mode cross section. The luminescence saturation method requires the knowledge of the radiation intensity distribution along the fibre radius, the relative profile of the distribution of Yb^{3+} ions over the fibre cross section, the lifetime of ions at the upper laser level, and the dependences of the relative luminescence intensity on the pump power in the fibre. It is important that the luminescence saturation method does not require the knowledge of the absolute concentration of Yb^{3+} ions, which is measured with an X-ray spectrometer with an insufficient accuracy in a number of cases.

The stimulated emission cross sections were obtained from luminescence spectra and the lifetime of Yb^{3+} ions at the upper laser level using the relation [9]

$$\sigma_e(\lambda) = \frac{\lambda^5}{8\pi c n^2 \tau} \frac{I(\lambda)}{\int \lambda I(\lambda) d\lambda}, \quad (1)$$

where c is the speed of light in vacuum; τ is the lifetime of the ion at the upper laser level; n is the refractive index of the material; and $I(\lambda)$ is the luminescence intensity. Integration is performed over the entire spectrum of the line of the transition under study.

To avoid the effect of reabsorption, we detected the luminescence intensity and lifetime in the direction perpendicular to the fibre axis. It is known that the observed lifetime does not always coincide with the radiative lifetime due to the possibility of nonradiative relaxation. However, in our case, the possibility of nonradiative transitions is virtually excluded because only one transition in Yb^{3+} ions is observed between the $^2F_{5/2}$ and $^2F_{7/2}$ levels in the visible range. In addition, the observation of luminescence in the measurements of the lifetime of Yb^{3+} ions at the upper laser level showed that the luminescence decay after pulsed excitation is described by a single exponential. The lifetimes of Yb^{3+} ions in PS and AS fibres were 1.45 and 0.83 ms, respectively. The scatter in the values of lifetimes measured in different fibres (AS and PS) of the same type (~ 4 %) lies within the experimental error.

The energy sublevels (Fig. 1) of the ground E_{1i} and excited E_{2j} states of Yb^{3+} ions were determined from the luminescence and absorption spectra of PS and AS fibres. Their energies are presented in Table 1.

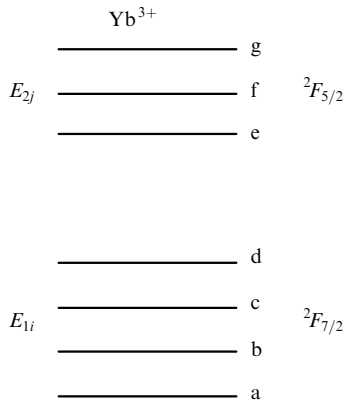

Figure 1. Energy level diagram of Yb^{3+}.

Table 1. Energies of the sublevels of Yb^{3+} in AS and PS fibre cores.

Level	Sublevel (Fig. 1)	Energy/cm^{-1}	
		PS fibre	AS fibre
$^2F_{7/2}$	a	0	0
	b	260	400
	c	440	760
	d	740	1210
$^2F_{5/2}$	e	10260	10245
	f	10520	10917
	g	10930	10940

The ratio of absorption and stimulated emission cross sections can be calculated from the sublevel energies as [9]

$$\sigma_e(\lambda) = \sigma_a(\lambda) \exp\left(\frac{\varepsilon - hc/\lambda}{kT}\right), \quad (2)$$

where h is Planck's constant; k is the Boltzmann constant; and T is the temperature. The value of ε can be found from the expression [9]

$$\exp\left(\frac{\varepsilon}{kT}\right) = \frac{\sum_j \exp[-E_{1i}/(kT)]}{\sum_i \exp[-E_{2j}/(kT)]}. \quad (3)$$

We determined experimentally the spectral dependences of stimulated transition cross sections in PS and AS fibres. Their maximum values are: $\sigma_a(974.5\ \text{nm}) = 1.4\ \text{pm}^2$, $\sigma_e(974.5\ \text{nm}) = 1.5\ \text{pm}^2$ in PS fibres and $\sigma_a(976\ \text{nm}) = 2.7\ \text{pm}^2$, $\sigma_e(976\ \text{nm}) = 3.0\ \text{pm}^2$ in AS fibres. The wavelengths of maxima of the stimulated emission and absorption cross sections virtually coincide (with the accuracy of 0.5 nm) for each of the glass types and are equal to 974.5 nm for the PS fibres and 976 nm for the AS fibres. The experimental ratio $\sigma_a(\lambda)/\sigma_e(\lambda)$ is in good agreement with (2), confirming the applicability of theory [2] to the calculation of transition cross sections for Yb^{3+} ions.

Figures 2 and 3 show the spectra of stimulated transition cross sections measured for PS and AS fibres, respectively. For comparison, the inset in Fig. 3 shows the spectra of transition cross sections for a germanosilicate glass obtained in [2]. One can see that stimulated transition cross sections for PS and AS fibres differ not only by their absolute values at the maximum (almost twice) but also by their spectra. Thus, the FWHM of the main peak of the absorption cross section in AS fibres is 7.7 nm, which is substantially greater than that in PS fibres (4.8 nm). As a result, the AS fibre lasers are less sensitive to changes in the pump wavelength (upon pumping to the main absorption peak) and, therefore, are more promising from this point of view. On the other hand, the absorption of AS fibres in the region from 930 to 970 nm is low, whereas PS fibres exhibit a plateau in this spectral region, which makes them more convenient when pumping is performed in this region. The difference in the absolute values of transition cross sections (the transition cross section in AS fibres is almost twice as high as that in PS fibres) can be more than compensated by the possibility of doping PS fibres with Yb^{3+} ions at concentrations approximately three times higher compared to AS fibres (owing to the doping methods developed at the Institute of Chemistry of High-Purity Materials, RAS (Nizhnii Novgorod) and Fiber Optics Research Center, A.M. Prokhorov General Physics Institute, RAS).

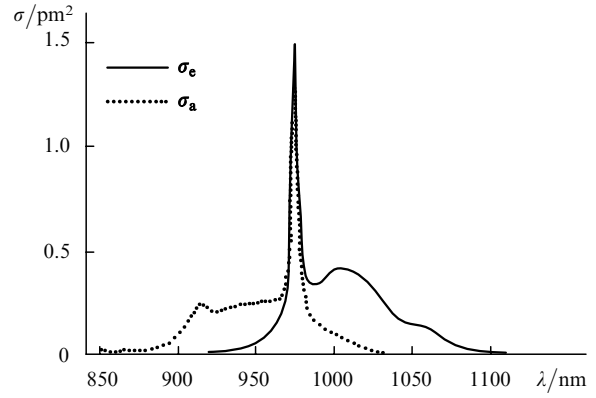

Figure 2. Spectral dependences of stimulated transition cross sections for Yb^{3+} in PS fibres.

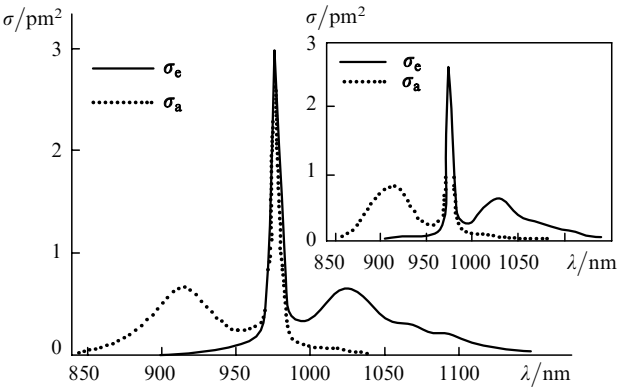

Figure 3. Same as in Fig. 2 for AS fibres. The inset shows the cross sections in a germanosilicate glass [2].

When developing Yb^{3+}-doped fibre lasers, one should bear in mind that the Yb^{3+}-doped AS and PS fibres have different spectral ranges of lasing because of different spectral dependences of the laser transition cross sections. This is especially manifested in the wavelength region (above 1100 nm), where the stimulated emission cross section in PS fibres is much lower that than in AS fibres (see Figs 2 and 3).

Knowing the dependences $\sigma_a(\lambda)$ and $\sigma_e(\lambda)$, we can calculate the lasing properties of fibre lasers. In particular, we determined spectral regions where efficient generation of double-clad Yb^{3+}-doped PS and AS fibre lasers can be obtained.

3. Emission spectral regions of double-clad Yb^{3+}-doped PS and AS fibre lasers

To obtain generation in the laser resonator at the wavelength λ, it is necessary to obtain the equality of the gain $G(\lambda)$ and optical losses $\gamma(\lambda)$ per round trip of radiation in the resonator at a certain pump level, provided that such a condition is not achieved for other wavelengths at lower pump levels (it is assumed that an efficient resonator exists for each wavelength).

Consider these conditions as applied to a standard double-clad, single-mode fibre laser with refractive-index fibre Bragg gratings (FBGs) as mirrors. The gain in the fibre cross section with the longitudinal coordinate z has the form

$$g(\lambda, z) = \sigma_e(\lambda)n_2(z) - \sigma_a(\lambda)n_1(z), \tag{4}$$

where n_1 is the concentration of the ground-state Yb^{3+} ions per unit volume; and n_2 is the concentration of the excited Yb^{3+} ions. Here, we neglect for simplicity the dependence of the gain on transverse coordinates. The total concentration of ytterbium ions per unit volume is n_0.

By representing the fraction of active ions at the upper level in the resonator as

$$\mu = \frac{\int_0^L n_2(z)\mathrm{d}z}{n_0 L}, \tag{5}$$

where L is the resonator length, we obtain that the gain per round trip in the resonator

$$G(\lambda) = 2[\sigma_e(\lambda) + \sigma_a(\lambda)]\mu n_0 L - 2\sigma_a(\lambda)n_0 L \tag{6}$$

at the lasing threshold should be equal to the radiation losses at the lasing wavelength: $G(\lambda) = \gamma(\lambda)$. Therefore, the fraction of ions at the upper level of the lasing threshold is

$$\mu(\lambda) = \frac{\sigma_a(\lambda)n_0 L + \gamma(\lambda)/2}{[\sigma_e(\lambda) + \sigma_a(\lambda)]n_0 L}. \tag{7}$$

By substituting into (7) the total losses per round trip in the resonator at a nonresonant (not coinciding with the Bragg wavelength) wavelength λ_{nr}, we find the wavelength $\gamma(\lambda_{nr})$ at which the function $\mu(\lambda_{nr})$ has a minimum $\mu^{min}(\lambda_{nr})$. Then, we substitute into (7) the losses at $\gamma(\lambda_r)$ at the resonant wavelength and again find the dependence $\mu(\lambda_r)$. It is obvious that lasing can be produced in the wavelength range where $\mu(\lambda_r) < \mu^{min}(\lambda_{nr})$. Therefore, knowing the product n_0L and losses $\gamma(\lambda_r)$ and $\gamma(\lambda_{nr})$ at the resonant and nonresonant wavelengths, we can find the emission range of the laser.

One can see from (7) that the lasing range is determined not only by losses per round trip in the resonator but also by the product n_0L. However, it is more convenient to calculate the design of a double-clad fibre laser by using another quantity, $\alpha_{cl}(\lambda_p)$, which is equal to the absorption coefficient for pump radiation from the first cladding over the entire length of the active fibre and is proportional to n_0L:

$$\alpha_{cl}(\lambda_p) = K\sigma_a(\lambda_p)n_0L, \tag{8}$$

where λ_p is the pump wavelength and K is the ratio of the areas of the fibre core and the first cladding. This expression is valid for fibres with the first cladding without a cylindrical symmetry. In the case of fibres with the first cladding in the form of a square with the 110-μm side and the core diameter 7.2 μm, the area ratio is $K \approx 1/300$.

We used the method for determining the lasing range considered above to estimate the possibilities of particular AS and PS fibre lasers. To increase the pump power coupled to the laser, we used GTWave fibres [13]. Fibres of this type represent two or more silica fibres placed inside a common reflecting polymer cladding with a low refractive index (see inset in Fig. 4). One of the fibres (active) has a core doped with ytterbium, while other silica fibres (passive) are in optical contact over the entire length with the first fibre and are used to couple pump radiation to the active fibre. The length of coupling between the passive fibre and the first cladding of the active fibre was measured to be ~0.5 m.

FBGs serving as resonator mirrors can be written at the ends of the active fibre or on the pieces of a special fibre spliced to the ends of the active fibre (Fig. 4).

The laser described here was based on a GTWave fibre consisted of two passive and one active fibres (with the PS core) placed inside a common reflecting cladding. From the point of view of absorption of pump radiation in the active fibre core, such a structure is virtually equivalent to a usual double-clad laser fibre, in which three cylindrical silica fibres play the role of the first cladding, the active fibre touching both passive fibres over the generatrix. This structure has no cylindrical symmetry, and therefore no additional efforts should be taken to provide efficient absorption of pump radiation in the active fibre core [14]. Each of the fibres had diameter 125 μm. The area ratio of the fibre core and first cladding was $K \approx 1/900$.

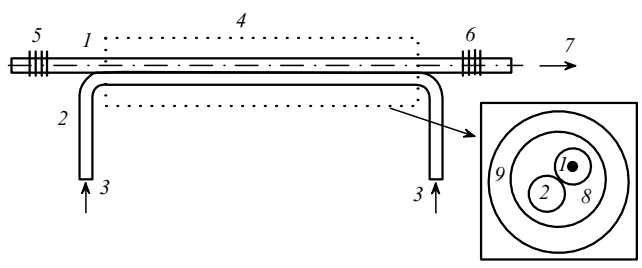

Figure 4. Scheme of the Yb-doped GTWave fibre laser: (*1*) active fibre; (*2*) passive fibre for pump coupling; (*3*) pump radiation; (*4*) GTWave fibre; (*5*) highly reflecting FBG; (*6*) FBG at the output end of the resonator; (*7*) output laser radiation. The inset shows the cross section of a double GTWave fibre: (*8*) reflecting polymer cladding; (*9*) protective jacket.

In the laser design in Fig. 4, different resonators can 'operate' at different wavelengths. Thus, at the lasing wavelength for which FBGs are calculated, the resonator losses are mainly determined by the reflection coefficient of the output FBG, which is usually chosen quite low (no more than 10 %) to achieve a high lasing efficiency. Therefore, losses at the wavelengths resonant for the FBG are ~10 dB. For other wavelengths, the role of the resonator can be performed, for example, by the fibre ends with the reflectivity ~3.5 % (losses per round trip in the resonator are ~29 dB). By using additional methods for feedback suppression (a skew end face of the fibre, immersion of the end face into a liquid with the refractive index close to that of silica, splicing with a multimode fibre, formation of a ball at the fibre end, etc.), one can further increase losses at each of the ends by ~20 dB. However, such methods are applicable only for the fibre end located behind the highly reflecting mirror and are difficult to realise for the output fibre end (except a skew end face) because in this case it is difficult to preserve single-mode output radiation. In long fibre lasers, backward scattering also plays an important role, which enhances a feedback. Therefore, it seems that it is difficult to obtain total losses per round trip in the resonator exceeding 49 – 50 dB at wavelengths near the laser wavelength.

To estimate the emission ranges of Yb^{3+}-doped PS and AS fibre lasers, we chose two combinations of losses per round trip of the resonant and nonresonant waves in the resonator. The first combination corresponds to a fibre laser whose resonator is formed by a highly reflecting FBG from one side and a perpendicular cleaved fibre end from the other side. There are no additional losses at the nonresonant wavelengths. In this case, losses per round trip in the resonator for the resonant wave are $\gamma(\lambda_r) = 14.5$ dB and for the nonresonant wave $\gamma(\lambda_{nr}) = 29$ dB. The second combination of losses corresponds to a fibre laser with the resonator formed by a highly reflecting FBG from one side and an additional FBG, as well as by a perpendicular cleaved fibre end from the other side, so that the losses per round trip of the resonant wave in the resonator are $\gamma(\lambda_r) = 10$ dB. In addition, the introduced additional losses at nonresonant wavelengths enhanced the total losses per round trip in the resonator for λ_{nr} up to $\gamma(\lambda_{nr}) = 49$ dB.

Based on the above values of $K^{I} = 1/300$ (for a single fibre) and $K^{III} = 1/900$ (for a triple fibre), we calculated the admissible lasing ranges for these two combinations of resonant and nonresonant losses as functions of total absorption of pump radiation from the first cladding in a single fibre (α_{cl}^{I}) and a triple fibre (α_{cl}^{III}). The results of calculations for PS and AS fibres are presented in Figs 5 and 6, respectively.

For comparison, the experimental point is presented in both figures, which corresponds to a triple GTWave fibre laser with the Yb-doped PS core. Absorption from the first

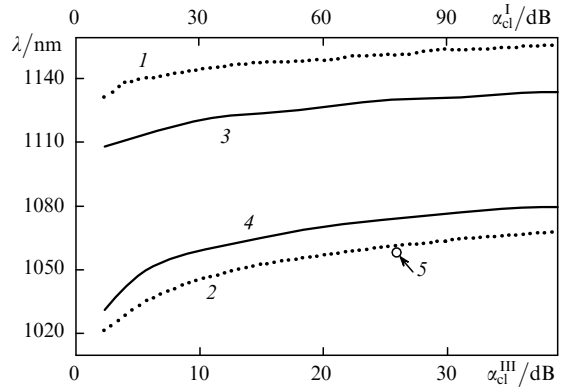

Figure 5. Possible emission range of the Yb-doped AS fibre laser as a function of the total absorption of the 976-nm pump radiation from the first cladding for a single (α_{cl}^{I}) and a triple fibre (α_{cl}^{III}) for two combinations of resonant and nonresonant losses: curves (*1*) and (*2*) are the upper and lower boundaries of the emission range for the combination of losses $\gamma(\lambda_r) = 10$ dB and $\gamma(\lambda_{nr}) = 49$ dB; curves (*3*) and (*4*) are the upper and lower boundaries of the emission range for the combination of losses $\gamma(\lambda_r) = 14$ dB and $\gamma(\lambda_{nr}) = 29$ dB; (*5*) experimental point.

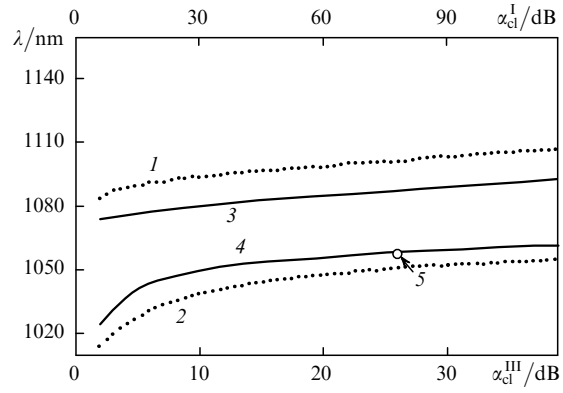

Figure 6. Same as in Fig. 5 for the Yb-doped PS fibre laser ($\lambda_p = 974.5$ nm).

cladding at the entire resonator length of 28 m was $\alpha_{cl}^{III}(974.5\ \text{nm}) = 26$ dB. A rather high total absorption was chosen because of the absence of thermal stabilisation of the pump source, which resulted in the temperature shift of the pump wavelength from 965 nm at a low power to 978 nm at the maximum power. In this case, the effective absorption of pump radiation was less than 26 dB, being within 25 % of low-power absorption. The absorption increased up to 65 % at the pump power equal to 3/4 of the maximum power and again decreased down to 40 % at the maximum power (taking into account the linewidth of the pump source). When the fibre laser length was shorter than 28 m, the lasing efficiency substantially decreased. This laser was intended for pumping a SRS radiation converter with the specified parameters, which required efficient lasing at 1058 nm.

One can see from Fig. 5 that the ytterbium-doped AS fibre laser can emit in the range from 1020 to 1155 nm, i.e., within a much broader wavelength range than ytterbium-doped PS fibre lasers (between 1015 and 1105 nm, Fig. 6). On the other hand, PS fibres make it possible to achieve lasing at shorter wavelengths. Thus, for the above-mentioned 25-dB absorption of pump radiation from the first cladding at 974.5 nm, it is impossible to obtain emission at 1058 nm in a triple AS fibre laser even for the combination of losses $\gamma(\lambda_r) = 10$ dB and $\gamma(\lambda_{nr}) = 49$ dB. At the same time, under the same conditions, a triple PS fibre laser can emit at this wavelength. In real experiments with PS fibre lasers, emission at 1058 nm (for $\alpha_{cl}^{III}(974.5\ \text{nm}) = 26$ dB) was obtained only by using a FBG at the resonator output and by suppressing radiation at nonresonant wavelengths. If the additional suppression of radiation is not used, then, according to calculations presented in Fig. 6, lasing cannot be obtained at a wavelength of 1058 nm. This is confirmed by the experiment – lasing appears not on the FBG but on fibre end faces at a wavelength of 1070 nm.

The dependences shown in Figs 5 and 6 were obtained in the approximation of the homogeneously broadened transition line. In reality, however, the inhomogeneous line broadening also exists, which can not only reduce the lasing efficiency but also cause lasing at two and more wavelengths.

For comparison, we present here the results obtained in paper [15], where the efficient lasing was obtained between 1049 and 1148 nm in ytterbium-doped AS fibres. The total absorption of pump radiation from the first cladding was $\alpha_{cl}^{I} = 22 - 40$ dB, and the fibre core diameter was $\sim$6 μm. Taking into account the difference between the area ratios for the fibre core and first cladding ($K = 1/300$ in our paper and $K \approx 1/430$ in [15]), the data [15] are in agreement with the results presented in Fig. 5.

Note that by pumping directly to the fibre core or the first cladding of a small diameter ($\sim$40 μm or smaller), or by decreasing the resonator length (displacement to the coordinate origin along the abscissa in Figs 5 and 6), lasing can be obtained at shorter wavelengths, down to 980 nm. This was performed, for example, in papers [16] and [17]. The efficient lasing at longer wavelengths can be achieved by heating the active fibre, thereby changing the laser transition cross section. Thus, lasing at 1180 nm was obtained by heating an ytterbium-doped fibre up to 70 °C [18].

4. Conclusions

We have measured the spectral dependences of cross sections for the stimulated $^2F_{5/2} - {}^2F_{7/2}$ transitions in Yb^{3+} ions in AS and PS fibres. The maximum cross sections are $\sigma_a(974.5\ \text{nm}) = 1.4\ \text{pm}^2$, $\sigma_e(974.5\ \text{nm}) = 1.5\ \text{pm}^2$ in PS fibres and $\sigma_a(976\ \text{nm}) = 2.7\ \text{pm}^2$, $\sigma_e(976\ \text{nm}) = 3.0\ \text{pm}^2$ in AS fibres. Based on the experimental data obtained, we calculated the possible emission ranges of Yb-doped double-clad PS and AS fibre lasers depending on the total absorption of pump radiation from the first cladding for different combinations of resonant and nonresonant losses.

Acknowledgements. The authors thank M.V. Yashkov (ICHPM, RAS) for fabricating fibre preforms, researchers of the group of S.V. Lavrishchev (FORC, GPI, RAS) for quantitative analysis of the fibre preforms, and M.E. Likhachev (FORC, GPI, RAS) for his help in measurements of the lifetime of the ytterbium laser level.

References

1. Pask H.M., Carman R.J., Hanna D.C., et al. *IEEE J. Sel. Topics Quantum Electron.*, **1**, 2 (1995).

2. Paschotta R., Nilsson J., Tropper A.C., Hanna D.C. *IEEE J. Quantum Electron.*, **33**, 1049 (1997).
3. Platonov N.S., Gapontsev D.V., Shumilin V. *CLEO'2002* (Long Beach, CA, 2002, CPDC3).
4. Gapontsev V., Krupke W. *Laser Focus World*, **38** (8), 83 (2002).
5. Nilsson J., Sahu J.K., Grudinin A.B., et. al. *Proc. SPIE Int. Soc. Opt. Eng.*, **4974**, 50 (2003).
6. Mao Y., Deng P., Gan F., et al. *Mater. Lett.*, **57**, 439 (2002).
7. Dai S., Sugiyama A., Hu L., et al. *J. of Non-Cryst. Solids*, **311**, 138 (2002).
8. Takebe H., Murata T., Morinaga K. *J. Am. Ceram. Soc.*, **79**, 681 (1996).
9. McCumber D.E. *Phys. Rev.*, **136**, A954 (1964).
10. Desurvire E. *Erbium-doped Fiber Amplifiers. Principles and Applications* (New York: John Wiley & Sons, 1994).
11. Melkumov M.A., Bufetov I.A., Kravtsov K.S., et al. *Preprint no. 5* (Moscow: FORC, GPI RAS, 2004).
12. Barnes W.L., Laming R.I., Tarbox E.J., Morkel P.R. *IEEE J. Quantum Electron.*, **27**, 1004 (1991).
13. Grudinin A.B., Turner P.W., Codemard C., et al. *ECOC'2002* (Copenhagen, Denmark, 2002) PD1.6.
14. Muendel M.H. *CLEO'1996, OSA Techn. Dig.* (Washington, DC, 1996) p. 209.
15. Kurkov A.S., Dianov E.M., Paramonov V.M., et al. *Kvantovaya Elektron.*, **30**, 791 (2000) [*Quantum Electron.*, **30**, 791 (2000)].
16. Kurkov A.S., Medvedkov O.I., Paramonov V.M., et al. *Proc. Conf. on Optical Amplifiers and Their Applications* (Stresa, Italy, 2001) OWC2.
17. Grudinin A.B., Nilsson J., Codemard C.A., et al. *Advanced Solid State Photonics 2003, Post deadline Presentations* (San Antonio, Texas, 2003) PD2.
18. Grukh D.A., Kurkov A.S., Paramonov V.M., Dianov E.M. *Kvantovaya Elektron.*, **34**, 579 (2004) [*Quantum Electron.*, **34**, 579 (2004)].